Journal of Mining and Environment (JME) Vol. 17, No. 5, 2026, 1675-1689

Shahrood University of Technology

Journal of Mining and Environment (JME)

Journal homepage: www.jme.shahroodut.ac.ir

Iranian Society of Mining Engineering (IRSME)

# Geomechanical and Joint-Density Controls on Blast Fragmentation: A Comparative Study of Precambrian Granitic Gneiss and Younger Granite Quarries, Plateau State, Nigeria

Ayobami Joshua Adegboye*, and Kayode Augustine Idowu

*Department of Mining Engineering, Faculty of Engineering, University of Jos, Jos, Plateau State, Nigeria*

***Article Info***

*Received 1 July 2026*

*Received in Revised form 3 August 2026*

*Accepted 5 September 2026*

*Published online 5 September 2026*

**DOI: 10.22044/jme.2026.17933.3570**

***Keywords***

*Blast fragmentation*

*Geomechanical properties*

*Granite*

*WipFrag*

*Uniaxial compressive strength*

***Abstract***

Quarry blasting in Plateau State, Nigeria, typically follows generic, site-unspecific designs that overlook the marked geological contrast between the Precambrian granitic gneiss of Mista Ali and the Younger Jurassic granite of Mararaba'n Jama'a. This study provides the first quantitative, ISRM-standardized comparison of intact-rock geomechanical properties, field-assessed joint density, and post-blast fragmentation between these two formations. Uniaxial compressive strength (UCS), Brazilian tensile strength (BTS), bulk density, specific gravity, and brittleness index were determined for ten specimens per site (n = 20). Post-blast fragmentation from two monitored production blasts per site was characterized by WipFrag image analysis. The Younger granite had significantly higher mean UCS (190.4 vs. 142.2 MPa) and BTS (15.4 vs. 10.3 MPa; $p < 0.001$, Cohen's $d > 4.3$), while field observation recorded predominantly sparse jointing at that site against dense jointing at the gneiss site. The gneiss site (powder factor 0.573 kg/m³) produced finer, more uniform fragmentation (X50 = 213 mm, n = 1.47) than the granite site (powder factor 0.495 kg/m³; X50 = 460 mm, n = 1.18), an association consistent with the combined influence of intact strength and joint density. UCS and BTS were near-perfectly correlated across the pooled dataset (r = 0.998). Because only two blasts were monitored per site, this is presented as a preliminary comparative case study rather than a statistically established causal relationship. The findings support trialing an increased powder factor (0.60–0.65 kg/m³) at the granite site and provide a mechanics-based geomechanical dataset currently scarce for African granite formations.

## 1. Introduction

Rock blasting is among the most critical and cost-intensive unit operations in quarrying, since the size and uniformity of the fragments produced directly govern the downstream costs of loading, hauling, crushing, and processing. Oversized boulders necessitate costly secondary blasting, while excessive fines represent wasted explosive energy and material loss. Achieving optimal fragmentation therefore requires a detailed understanding of how a given rock mass responds to explosive loading.

Nigeria possesses extensive granite deposits that form the primary source of construction aggregate across the country. Within Plateau State, two geologically distinct granite suites are of particular economic importance: the Precambrian Basement Complex granitic gneisses of the Bassa area (Mista Ali axis), formed approximately 600 million years ago through Pan-African orogenesis [1,2], and the Younger Jurassic ring-complex granites of the Mararaba'n Jama'a axis along the Jos Plateau, emplaced roughly 150 to 170 million years ago [3]. These suites differ markedly in mineralogy, texture, and degree of jointing, yet quarry operators across the region largely apply

*Corresponding author: adegboyea@unijos.edu.ng (A. J. Adegboye)*

generic blast designs that do not account for these site-specific geomechanical conditions. The result is persistent fragmentation inconsistency, frequent secondary blasting, and inefficient use of explosive energy.

Internationally, uniaxial compressive strength (UCS), Brazilian tensile strength (BTS), and brittleness index have been shown to be primary determinants of blast fragment size [4–7,30]. It is well recognized, however, that intact-rock strength is not the only control on fragmentation: rock-mass-scale blastability descriptors, including rock mass description (RMD), joint plane spacing (JPS), joint plane orientation (JPO), and specific gravity influence (SGI), as formalized in Lilly's blastability index [14] and subsequently applied to jointed rock masses elsewhere [23], with the fragmentation influence of pre-existing discontinuities also demonstrated experimentally in granitic rock [31], capturing discontinuity-controlled behavior that intact-specimen testing alone cannot represent. The present study's field joint-density assessment (Section 2.2) is a simplified, qualitative proxy for these rock-mass-scale descriptors rather than a full blastability index; this is an acknowledged limitation, discussed further in Section 3.1. However, comparable quantitative studies on Nigerian granites remain scarce. Existing Nigerian quarry studies [8–10] have examined fragmentation within isolated quarry settings, while [11], although addressing rock discontinuity parameters for blast performance prediction in Nigerian quarries, did not establish a comparative geomechanical framework across geologically distinct granite formations; none combines paired intact-rock and rock-mass characterization with field fragmentation monitoring across two contrasting granite suites in the manner attempted here. This paired intact-rock/rock-mass, dual-formation comparative framework, rather than any single measured parameter, constitutes the specific novelty of the present work relative to earlier Nigerian quarry studies. Recent work elsewhere continues to refine empirical and data-driven fragmentation prediction, including measurement-based blast-plan optimization frameworks [24,26], updated empirical fragmentation models for jointed rock masses [25], and machine-learning-based approaches to powder factor prediction and optimization [27,29]; these are revisited in Section 3.4 as candidate tools for future refinement of the site-specific recommendations proposed here. A companion study has already contrasted the unit production economics of the two quarries investigated here [12], underscoring the operational relevance of the present geomechanical investigation. The well-established importance of geomechanical properties in controlling blast outcomes [13–15], combined with the near-complete absence of such data for Plateau State granites, and the availability of empirical fragmentation models such as Kuz-Ram, originating from Kuznetsov's pioneering work [16] and later formalized by Cunningham [17], against which site-specific behavior can be benchmarked, together justify this study.

Addressing this specific gap, the present study determined how key intact-rock geomechanical properties and field-assessed joint density of the Precambrian granitic gneiss (Jolex Construction Company, Mista Ali) and the Younger Jurassic granite (Afrimine Construction Company, Mararaba'n Jama'a) are associated with post-blast fragmentation outcomes, and used these relationships to derive preliminary, practical, site-specific blast design guidance for these formations. Specifically, the study (i) determined and compared the intact geomechanical properties of fresh granite specimens from the two sites; (ii) quantified and compared post-blast fragmentation outcomes from production blasts at each site; (iii) established empirical relationships among the measured geomechanical properties; and (iv) proposed preliminary, engineering-judgment-based optimized, site-specific blast design parameters for validation through further monitored trial blasting.

## 2. Materials and Methods

To meet the objectives outlined above, the methodology combined ISRM-standardized intact-rock laboratory testing with field-based joint-density assessment and WipFrag digital image analysis of production blasts, enabling evaluation of intact-rock strength, rock-mass jointing, and fragmentation outcomes on a common, comparable basis at both sites. The following subsections describe, in turn, the study area, sample collection and laboratory testing, blast fragmentation analysis, and the

statistical treatment applied to the resulting dataset.

### 2.1. Study area

The study was conducted at two active granite quarries in Plateau State, north-central Nigeria (Figure 1). The first site is the Precambrian granitic gneiss quarry of Jolex Construction Company (JCC), Mista Ali, Bassa Local Government Area (latitude N10°02'44", longitude E08°51'20" to E08°51'24"). The second is the Younger Jurassic granite quarry of Afrimine Construction Company, Mararaba'n Jama'a, Jos South Local Government Area, along Zaria Road (latitude N09°40'00" to N09°44'00", longitude E08°51'00" to E08°55'00"). Both sites were in active production at the time of data collection.

The JCC Mista Ali rock is a foliated, medium- to coarse-grained granitic gneiss of the Precambrian Basement Complex, formed through Pan-African orogenesis approximately 600 million years ago [1,2]; its mineralogy is dominated by quartz, plagioclase, and alkali feldspar, with biotite and minor hornblende defining a pervasive gneissic foliation. The rock mass is cut by multiple, closely spaced foliation-parallel and cross-cutting joint sets that impart the dense discontinuity network described in Section 3.1. The Afrimine Mararaba'n Jama'a rock is a younger (Jurassic) ring-complex granite, emplaced as a post-orogenic, largely undeformed pluton approximately 150 to 170 million years ago [3]; it is coarser-grained, massive, and equigranular, dominated by alkali feldspar (including perthite), quartz, and subordinate biotite, and lacks the tectonic foliation of the Basement Complex gneiss, consistent with its comparatively sparse, widely spaced jointing. These contrasting emplacement histories, textures, and structural fabrics provide the geological basis for the intact-strength and joint-density contrasts examined in this study.

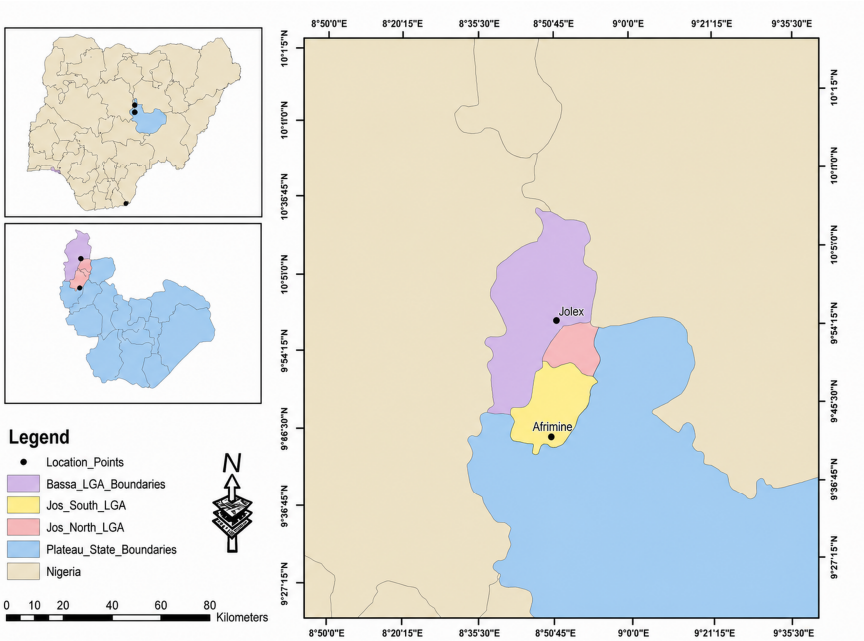


**Figure 1. Location map of the two study quarry sites (Jolex Construction Company, Mista Ali, and Afrimine Construction Company, Mararaba'n Jama'a) in Plateau State, Nigeria.**

### 2.2. Sample collection and laboratory testing

Ten fresh, unweathered granite block samples (minimum 30 cm × 30 cm × 30 cm) were collected from active benches at each site, avoiding blast-disturbed or weathered zones. Ten specimens per site were selected as double the minimum of five specimens per test recommended by ISRM (2007) Suggested Methods [18] for determining a representative mean and variance, in order to improve the precision of the between-site comparison; this sample size was set a priori on this basis rather

than through a formal statistical power calculation, and the coefficients of variation subsequently obtained (5.8–10.6%; Section 3.1) indicate that adequate within-site precision was achieved for the parameters measured, though this does not by itself demonstrate that ten specimens is the statistically optimal sample size. Joint density, an intrinsically rock-mass-scale (rather than intact-specimen-scale) property, was assessed qualitatively in the field by visual estimation of discontinuity spacing against a 1 m scale reference at ten observation zones per site and categorized as sparse (mean spacing > 1 m), moderate (0.3–1 m), or dense (< 0.3 m); no quantitative scanline or window mapping was performed, and this qualitative assessment should be understood as an indicative characterization of rock-mass structure rather than a full discontinuity survey or blastability index. Cylindrical specimens for UCS testing (diameter D ≥ 50 mm, length-to-diameter ratio 2.5:1) and Brazilian disc specimens for BTS testing (D ≥ 50 mm, thickness t = 0.5D) were prepared by diamond sawing and grinding to ISRM (2007) Suggested Methods tolerances [18] (Figure 2).

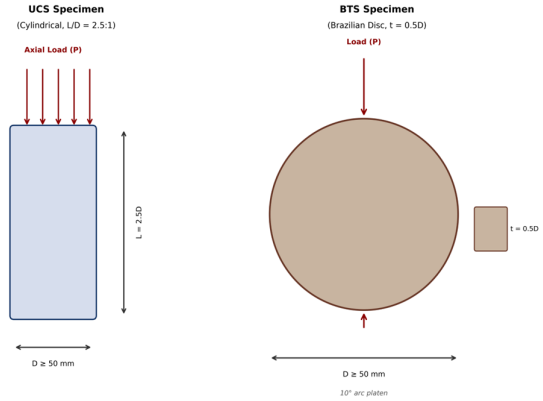


**Figure 2. Specimen preparation for UCS and BTS testing: cylindrical UCS specimen (L/D = 2.5:1, D ≥ 50 mm) (left) and Brazilian disc specimen (t ≈ 0.5D) (right).**

Bulk density and specific gravity were determined from oven-dried and water-saturated/suspended weights (ρb = Wdry / (Wdry − Wsub)). UCS specimens were loaded axially at 0.5 to 1.0 MPa/s; BTS specimens were loaded diametrically at 0.2 MPa/s using a jig with 10° arc loading platens, with BTS = 2P / (πDt), where P is the peak load, D is the specimen diameter, and t is the specimen thickness. Brittleness index was calculated as BI = (UCS − BTS) / UCS.

### 2.3. Blast fragmentation analysis

Two production blasts were monitored at each site (four blasts in total). For each blast, burden, spacing, hole depth, hole diameter, explosive charge, stemming length, initiation sequence, and powder factor were recorded. Both quarries employed the same bottom-primed explosive configuration and initiation practice typical of Nigerian aggregate-quarry blasting: a cartridged emulsion explosive (Superpower 90 or Solar Gel) was placed at the bottom of each blast hole to serve as a high-energy primer/booster, with the remainder of the column charged with ANFO (ammonium nitrate/fuel oil), a lower-cost bulk explosive used to fracture the main granite body economically. This emulsion-primed, ANFO-filled charging configuration was applied consistently at both sites and was not systematically varied between blasts; therefore, explosive type is treated here as a controlled background variable rather than a source of between-site variability. Calibrated photographs of the post-blast muck pile (minimum two per blast, eight images in total across the four blasts, with a 300 mm × 300 mm scale card placed in the foreground) were taken immediately after blasting, before any disturbance of the blasted rock, from multiple vantage points around the accessible faces of the muck pile to reduce bias toward any single face. Images were captured using a Nikon D3500 DSLR camera (24.2 megapixels, approximately 6000 × 4000 pixel resolution) with an 18–55 mm lens and processed in WipFrag (version 4.0) [19]. The images were calibrated against the in-frame scale card, and particle boundaries generated by the automatic edge-detection algorithm were reviewed and manually corrected where fines were obscured or boundaries were ambiguous, following standard WipFrag procedures; the proportion of boundaries requiring manual correction was not systematically logged or quantified during processing. Quantifying this proportion is recommended for future monitoring campaigns at these sites. All images were processed by the same analyst (the corresponding author) using a consistent settings protocol; however, a formal repeatability check (e.g., re-processing a

subset of images to quantify operator-dependent variability) was not conducted and is recommended for future monitoring campaigns at these sites. WipFrag output was used to derive the Rosin-Rammler cumulative percent-passing curve, from which the mean fragment size (X50, the screen size corresponding to 50% passing) and the uniformity index (n) were obtained; n describes the slope of the Rosin-Rammler distribution, $R(x) = 100 \times \exp[-0.693(x/X50)^n]$, with larger n indicating a more uniform fragment size distribution and smaller n indicating a wider spread including fines and oversize. WipFrag output also reports X10 and X80 (the screen sizes corresponding to 10% and 80% cumulative passing) for each blast; these are tabulated alongside X50 and n in Table 2 and discussed in Section 3.2. An oversize fraction relative to a defined secondary-breakage threshold and intermediate percentiles such as X20 were not separately extracted from the WipFrag output and are recommended as additional metrics for future monitoring campaigns at these sites.

### 2.4. Statistical analysis

Descriptive statistics (mean, standard deviation, coefficient of variation) were computed for all geomechanical variables, with a coefficient of variation below 15% adopted as an indicative reliability threshold rather than a formal sample size justification (see Section 2.2). Normality of each variable within each site was assessed by inspection of skewness and the Shapiro-Wilk statistic, and equality of variance between sites was tested with Levene's test; where variances were unequal, Welch's t-test was used instead of the pooled-variance t-test, and this is noted in the relevant results. Differences between sites were tested using independent-samples t-tests ($\alpha = 0.05$) and are reported alongside 95% confidence intervals for the mean difference and Cohen's d as a standardized effect size, allowing the distinction between statistical and practical significance (Section 3.1). Pearson correlation and simple linear regression were employed to examine relationships among the 20 intact rock specimens; because this pooled dataset spans two distinct site populations with non-overlapping strength ranges, the resulting correlation coefficient reflects both the within-site relationship between UCS and BTS and the between-site separation in mean strength. This distinction is explicitly discussed in Section 3.3 rather than treating the pooled correlation as evidence of a relationship within a single population. Given the limited blast dataset (n = 4), inferential testing of fragmentation outcomes was not performed; instead, site-level geomechanical trend analysis and descriptive comparisons were used, consistent with [20,21]. The resulting fragmentation comparison is presented throughout as a site-level association appropriate for a preliminary comparative case study rather than as a statistically established causal relationship.

## 3. Results and Discussion

### 3.1. Intact rock geomechanical properties and between-site comparison

Table 1 summarises the descriptive statistics, independent-samples t-test results, 95% confidence interval of the difference and Cohen's d effect size for intact rock properties at the two sites (degrees of freedom = 18 throughout, pooled-variance test; Levene's test did not indicate significant heteroscedasticity for any variable, so Welch correction was not required). UCS averaged 142.2 MPa (standard deviation 8.2; coefficient of variation 5.8%) at JCC Mista Ali against 190.4 MPa (standard deviation 11.0; coefficient of variation 5.8%) at Afrimine Mararaba'n Jama'a, a 48.2 MPa (34%) difference ($t = 11.13$, $p < 0.001$, 95% CI of the difference 39.1 to 57.3 MPa, Cohen's d ≈ 5.0). BTS averaged 10.3 MPa at JCC against 15.4 MPa at Afrimine, a 50% margin ($t = 9.72$, $p < 0.001$, 95% CI 4.0 to 6.2 MPa, Cohen's d ≈ 4.35). Bulk density and specific gravity were also significantly higher at Afrimine (bulk density: $t = 6.71$, $p < 0.001$, 95% CI 0.041 to 0.079 g/cm³, Cohen's d ≈ 3.0; specific gravity: $t = 8.86$, $p < 0.001$, 95% CI 0.045 to 0.075, Cohen's d ≈ 3.96), consistent with denser rock generally being stronger. The very large effect sizes obtained for all five parameters indicate that these between-site differences are not only statistically significant but also large relative to within-site variability, which supports treating them as practically, and not merely statistically, meaningful. All within-site coefficients of variation were below 15% (and below 11% for all parameters except BTS at JCC, 10.6%), indicating adequate within-site measurement precision at the sample size

used; this precision does not, on its own, establish that ten specimens is a statistically optimal or externally validated sample size (Section 2.2).

**Table 1. Descriptive statistics and independent-samples t-test results for intact rock properties at the two quarry sites (n = 10 per site; degrees of freedom = 18).**

| Parameter | JCC Mean (SD) | JCC CV (%) | Afrimine Mean (SD) | Afrimine CV (%) | t-stat | p-value | 95% CI of Difference | Cohen's d |
|---|---|---|---|---|---|---|---|---|
| Bulk Density (g/cm³) | 2.62 (0.02) | 0.8 | 2.68 (0.02) | 0.7 | 6.71 | < 0.001 | 0.041 to 0.079 | 3.00 |
| Specific Gravity | 2.66 (0.01) | 0.5 | 2.72 (0.02) | 0.7 | 8.86 | < 0.001 | 0.045 to 0.075 | 3.96 |
| UCS (MPa) | 142.2 (8.2) | 5.8 | 190.4 (11.0) | 5.8 | 11.13 | < 0.001 | 39.1 to 57.3 | 4.97 |
| BTS (MPa) | 10.3 (1.1) | 10.6 | 15.4 (1.3) | 8.1 | 9.72 | < 0.001 | 4.0 to 6.2 | 4.35 |
| Brittleness Index | 0.928 (0.004) | 0.4 | 0.919 (0.002) | 0.2 | -6.66 | < 0.001 | 0.006 to 0.011 | -2.98 |
| UCS/BTS Ratio | 13.83 (0.66) | 4.8 | 12.36 (0.30) | 2.4 | n/a | n/a | n/a | n/a |

Note: The UCS/BTS ratio was not subjected to t-testing because it is a derived ratio computed from the primary variables (UCS and BTS), which were already tested independently; the ratio is presented for comparative reference only. Bulk density, specific gravity, and UCS/BTS ratio are reported to two decimal places, and UCS and BTS to one decimal place, matching the resolution of the corresponding laboratory instrumentation. The brittleness index is reported to three decimal places because it is a dimensionless ratio close to 1.0, for which the between-site difference is only resolved at that precision. The 95% CI of the difference and Cohen's d were computed from the pooled standard deviation and each site's mean, SD, and n = 10 using standard two-sample formulas (df = 18, t-critical = 2.101). The negative sign for the brittleness index reflects the direction of the mean difference (JCC > Afrimine), whereas the positive values for the other parameters reflect Afrimine > JCC

Brittleness index was calculated as BI = (UCS − BTS)/UCS (Section 2.2), following the same formulation used in prior fragmentation-oriented brittleness studies [22], under which values approaching 1.0 indicate a rock in which tensile strength is a small fraction of compressive strength and which is therefore classified, on the conventional qualitative scale applied in that literature, as "highly brittle" above approximately BI = 0.85–0.90; both formations exceed this threshold. Although both formations are consequently classified as highly brittle (BI > 0.90), the Afrimine granite showed a slightly but statistically significantly lower brittleness index (0.919 vs. 0.928, t = -6.66, p < 0.001, 95% CI of the difference 0.006 to 0.011), reflecting a marginally higher BTS/UCS ratio (approximately 0.081 vs. 0.072). The absolute magnitude of this difference (0.009 BI units) is small, and given that BI enters no established quantitative fragmentation model used in this study, its practical contribution to the observed fragmentation contrast should be regarded as secondary to, and considerably smaller than, the absolute UCS and BTS differences discussed above; it is reported here primarily for completeness and comparability with other brittleness-based studies, rather than as a major explanatory variable. Because blast-induced rock breakage is governed primarily by tensile fracture [28], a formation with proportionally greater tensile resistance relative to its compressive strength is harder to fragment per unit of explosive energy even where its compressive strength is simply higher; on this basis, the Afrimine granite presents a somewhat compounded resistance to fragmentation, being both absolutely stronger and marginally more tensile-resistant in proportional terms than the JCC gneiss, though the absolute UCS and BTS contrasts remain the dominant intact-rock factors.

This intact-strength contrast is reinforced by structural differences observed in the field. Joint density was recorded as dense (estimated spacing < 0.3 m) in 7 of 10 observation zones at JCC, against sparse jointing (estimated spacing > 1 m) in 7 of 10 zones at Afrimine. Mean UCS and BTS comparisons with standard deviation error bars (Figures 3 and 4) illustrate the clear separation between sites, with negligible overlap in either parameter.

### 3.2. Blast fragmentation outcomes

Table 2 presents the blast design parameters and WipFrag fragmentation results for the four monitored production blasts. The two JCC blasts produced X50 values of 216 mm and 210 mm (mean 213 mm) and uniformity index values of 1.51 and 1.42 (mean 1.47) at powder factors of 0.560 and 0.585 kg/m³ (Figures 5 and 6). The two Afrimine blasts produced substantially coarser X50 values of 485 mm and 435 mm (mean 460 mm) and lower uniformity index values of 1.08 and 1.28 (mean 1.18) at lower powder factors of 0.480 and 0.510 kg/m³ (Figures 7 and 8). The comparison across all four blasts is summarised in Figures 9 and 10. The Afrimine uniformity index values lie close to the 1.1–1.2 range reported for WipFrag-analysed granite aggregate quarry blasts elsewhere [19], lending external support to the present measurements, while the comparatively higher JCC values reflect the additional

fragmentation contribution from dense in-situ jointing at that site. The X10–X80 spread reinforces this pattern: at JCC the fine and coarse ends of the distribution are close together (mean X10 = 53.0 mm, X80 = 434.8 mm, a ratio of about 8), consistent with the tight, jointing-controlled fragmentation implied by the high uniformity index, whereas at Afrimine the distribution is far more spread out (mean X10 = 80.0 mm, X80 = 1130.3 mm, a ratio of about 14), with a X80 approaching or exceeding 1 m in both blasts, indicating a substantial oversize tail that would be expected to require secondary breakage before crushing.

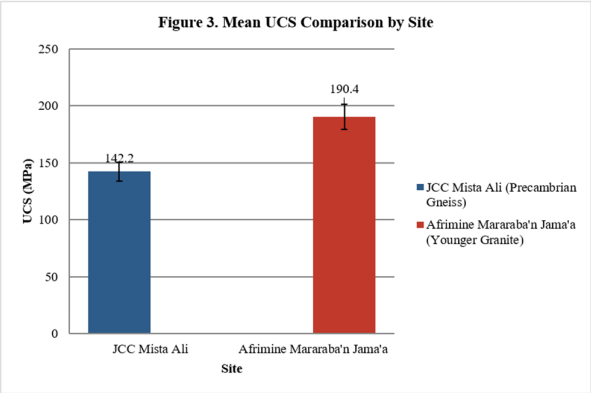


**Figure 3. Mean UCS comparison (± 1 SD) between JCC Mista Ali and Afrimine Mararaba'n Jama'a (n = 10 per site).**

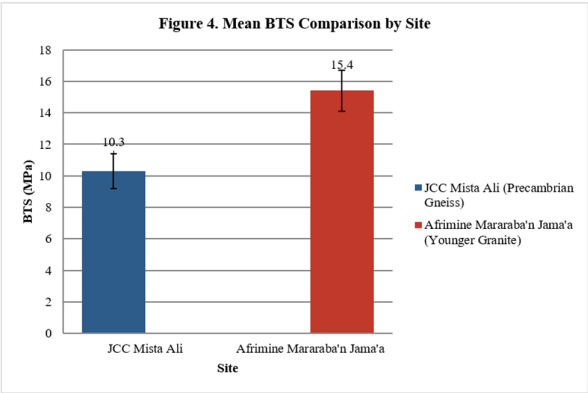


**Figure 4. Mean BTS comparison (± 1 SD) between JCC Mista Ali and Afrimine Mararaba'n Jama'a (n = 10 per site).**

**Table 2. Blast design parameters and WipFrag fragmentation outcomes for the four production blasts (B = burden, S = spacing, H = hole depth, d = hole diameter, PF = powder factor, X10/X80 = screen size corresponding to 10%/80% cumulative passing).**

| Blast ID | Quarry | B (m) | S (m) | H (m) | d (mm) | PF (kg/m³) | X10 (mm) | X50 (mm) | X80 (mm) | n |
|---|---|---|---|---|---|---|---|---|---|---|
| JCC-B01 | JCC Mista Ali | 3.05 | 3.25 | 10.20 | 89 | 0.560 | 57.2 | 216 | 448.8 | 1.51 |
| JCC-B02 | JCC Mista Ali | 3.12 | 3.30 | 9.85 | 89 | 0.585 | 48.9 | 210 | 420.8 | 1.42 |
| JCC Mean | — | 3.09 | 3.28 | 10.03 | 89 | 0.573 | 53.0 | 213 | 434.8 | 1.47 |
| AFR-B01 | Afrimine Mararaba'n Jama'a | 2.95 | 3.15 | 10.40 | 89 | 0.480 | 60.2 | 485 | 1140.1 | 1.08 |
| AFR-B02 | Afrimine Mararaba'n Jama'a | 2.88 | 3.10 | 9.90 | 89 | 0.510 | 99.8 | 435 | 1120.6 | 1.28 |
| Afrimine Mean | — | 2.92 | 3.13 | 10.15 | 89 | 0.495 | 80.0 | 460 | 1130.3 | 1.18 |

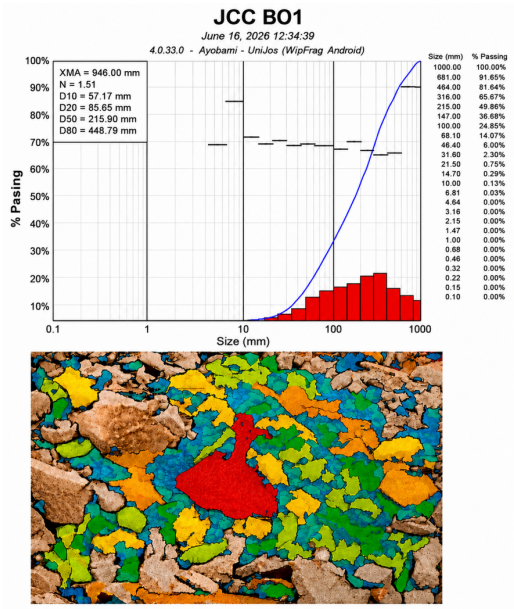


**Figure 5. WipFrag fragmentation analysis for blast JCC-B01, JCC Mista Ali (Rosin-Rammler cumulative percent-passing curve and fragmentation statistics).**

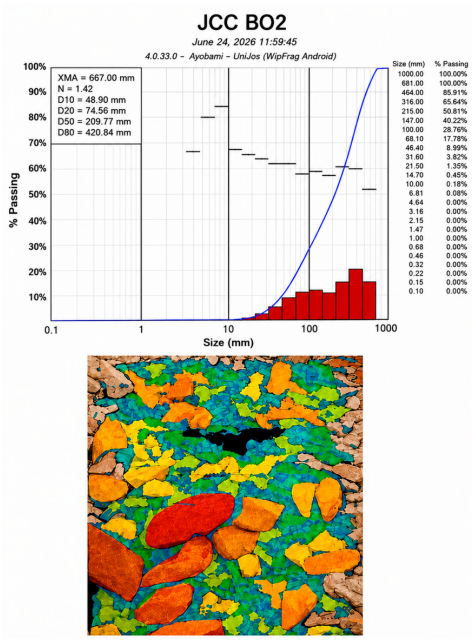


**Figure 6. WipFrag fragmentation analysis for blast JCC-B02, JCC Mista Ali.**

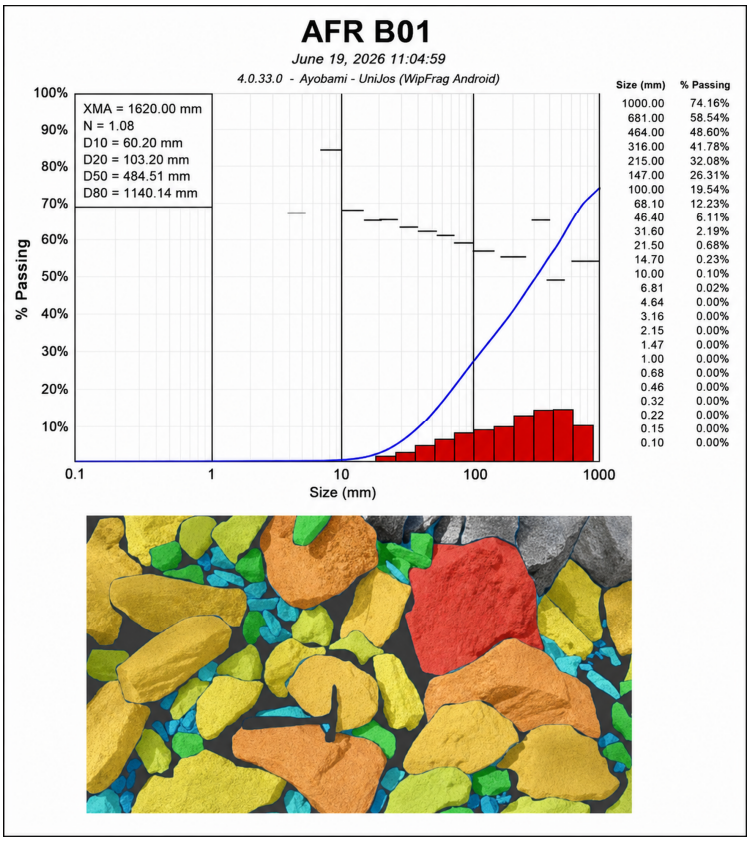


**Figure 7. WipFrag fragmentation analysis for blast AFR-B01, Afrimine Mararaba'n Jama'a.**

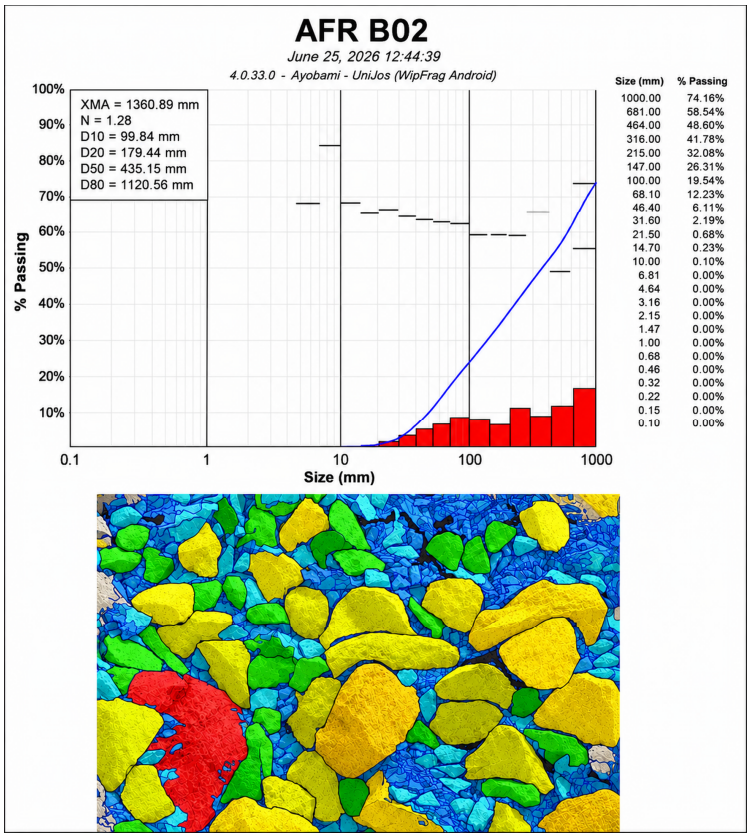


**Figure 8. WipFrag fragmentation analysis for blast AFR-B02, Afrimine Mararaba'n Jama'a.**

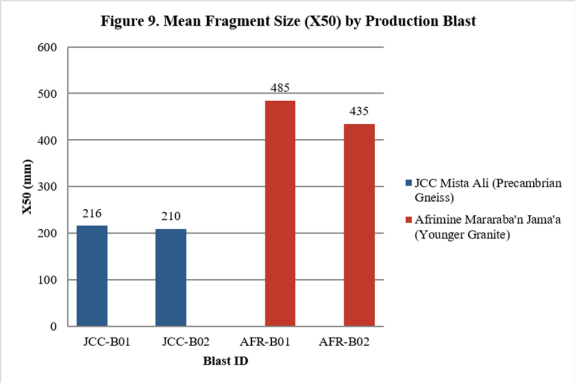


**Figure 9. Comparison of mean fragment size (X50, mm) across all four production blasts.**

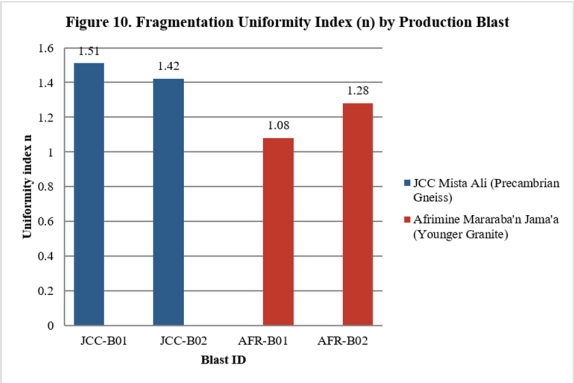


**Figure 10. Comparison of fragmentation uniformity index (n) across all four production blasts.**

This pattern aligns with the general blasting principle that a higher powder factor produces finer fragmentation, since JCC achieved finer fragmentation at a higher mean powder factor (0.573 kg/m³) than Afrimine (0.495 kg/m³). This raises the question of whether the fragmentation contrast could be solely attributed to the powder factor difference, rather than to the contrasting intact-rock strength and joint density emphasized above; however, the relationship between powder factor and fragment size holds only when rock mass conditions are broadly comparable, and the two formations differ too substantially in strength and jointing for powder factor alone to be a sufficient explanation. At JCC, the dense joint network provides a pre-existing structural template along which blast-induced stress can propagate [31], so a moderate powder factor suffices to produce fine, uniform fragmentation and high repeatability between blasts (X50 range of only 6 mm). At Afrimine, sparse jointing offers few natural planes of weakness, so the explosive must fracture largely intact, high-strength rock; the applied powder factor of 0.495 kg/m³ is consequently insufficient, producing coarse, irregular fragments and greater between-blast variability (X50 range of 50 mm). The geomechanical contrast between the two formations, rather than powder factor in isolation, is therefore the dominant control on the fragmentation difference observed. Blast geometry could, in principle, also contribute to this contrast, so it is useful to examine whether the recorded design parameters could independently explain it. As shown in Table 2, mean burden and spacing were, if anything, marginally smaller at Afrimine (2.92 m and 3.13 m) than at JCC (3.09 m and 3.28 m), and mean hole depth was closely comparable between sites (10.15 m versus 10.03 m); a smaller burden and spacing would conventionally be expected to promote, not hinder, fine fragmentation. Stemming length and explosive charge distribution were held to standard practice at both sites and were not systematically varied in this dataset. The observed direction of the fragmentation contrast is therefore opposite to what would be predicted from burden and spacing alone, which reinforces, rather than confounds, the interpretation that intact-rock strength and joint density are the dominant controls; a fully factorial analysis that formally partitions the contributions of geometry, powder factor, and rock properties was beyond the scope of the present four-blast dataset and is recommended for future work with a larger number of monitored blasts.

### 3.3. Empirical relationships among geomechanical properties

Table 3 presents the Pearson correlation matrix for the combined 20-specimen dataset. UCS and BTS were almost perfectly correlated ($r = 0.998$, $p < 0.01$), and the simple linear regression BTS = -5.04 + 0.108 × UCS explained 99.5% of the variance in BTS ($R^2 = 0.995$, $p < 0.001$; Table 4, Figure 11). Because this correlation is computed on a pooled dataset comprising two distinct site populations with non-overlapping UCS ranges (approximately 130–155 MPa at JCC and 175–210 MPa at Afrimine), part of the very high pooled r reflects the clear separation between site means rather than a purely within-population relationship; the low within-site coefficients of variation for both UCS and

BTS (Table 1) indicate that each site's data cluster tightly, which is also consistent with a genuine linear relationship holding within each population, but the present dataset, with only ten specimens per site spanning a comparatively narrow strength range at each site, is not able to fully separate the within-site slope from the between-site offset. This distinction does not affect the paper's central use of the UCS-BTS relationship as an internal consistency check on the laboratory dataset, but it should be kept in mind before extrapolating the fitted regression to other granite formations with different mean strength levels. Bulk density correlated strongly with both UCS (r = 0.976) and BTS (r = 0.984), and brittleness index correlated negatively with all strength parameters.

**Table 3. Pearson correlation matrix for intact rock mechanical properties (n = 20; ** p < 0.01, two-tailed).**

| Property | Bulk Density | UCS (MPa) | BTS (MPa) | BI |
|---|---|---|---|---|
| Bulk Density | 1.000 | 0.976** | 0.984** | -0.976** |
| UCS (MPa) | 0.976** | 1.000 | 0.998** | -0.958** |
| BTS (MPa) | 0.984** | 0.998** | 1.000 | -0.974** |
| BI | -0.976** | -0.958** | -0.974** | 1.000 |

**Table 4. Simple linear regression results: BTS and brittleness index (BI) as functions of UCS (n = 20).**

| Regression Model | Intercept (a) | Slope (b) | $R^2$ | p-value |
|---|---|---|---|---|
| BTS = a + b(UCS) | -5.04 | 0.108 | 0.995 | < 0.001 |
| BI = a + b(UCS) | 0.954 | -0.000187 | 0.917 | < 0.001 |

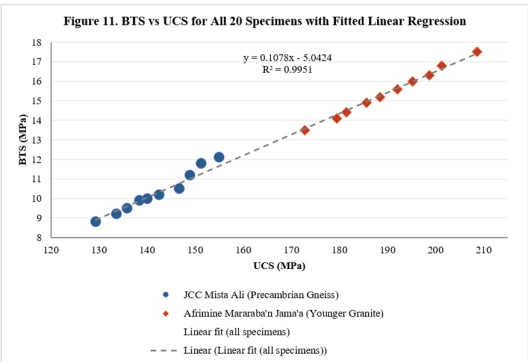


**Figure 11. Scatter plot of BTS (MPa) versus UCS (MPa) for all 20 specimens with fitted linear regression trendline.**

The UCS/BTS ratio averaged 13.83 at JCC and 12.36 at Afrimine, both within the range of 10 to 15 reported for fresh crystalline granites [22], supporting the reliability of the laboratory dataset. Beyond serving as a plausibility check, the UCS/BTS ratio is relevant to fragmentation because it summarizes the balance between compressive and tensile resistance that a blast must overcome: a lower ratio, as observed at Afrimine, indicates a proportionally larger tensile component relative to compressive strength, consistent with the slightly lower brittleness index at that site (Section 3.1), while a higher ratio, as at JCC, indicates a rock in which tensile failure is comparatively easier to initiate relative to its compressive strength. Because blast fragmentation is predominantly a tensile-failure process, the higher UCS/BTS ratio at JCC is consistent with, and reinforces, the observation that JCC fragments more readily despite its lower absolute strength. Taken together with the near-identical intercept and slope of the pooled UCS-BTS regression, these results indicate that UCS and BTS measure a common underlying strength characteristic within these formations, and that the 48.2 MPa UCS gap and 5.1 MPa BTS gap between sites represent a substantial, geomechanically meaningful contrast in the energy required to initiate and propagate fracture in each rock type, rather than measurement noise.

### 3.4. Implications for site-specific blast design

Table 5 consolidates the geomechanical and fragmentation findings at site level, and Table 6 sets out preliminary, engineering-judgement-based blast design recommendations derived from these relationships. These recommendations were not generated by a formal optimisation algorithm or by inverting a calibrated fragmentation model against target X50 values; rather, they represent conservative, directional adjustments to the existing design parameters, informed by the observed magnitude of the intact-strength contrast, the qualitative joint-density contrast,

and standard blasting engineering practice (e.g., increasing powder factor and reducing burden for stronger, more sparsely jointed rock, and vice versa), and are explicitly intended as calibration starting points for trial blasting rather than finalised design values (Section 3.4, final paragraph).

**Table 5. Site-level geomechanical and fragmentation summary comparison.**

| Parameter | JCC Mista Ali (Precambrian Gneiss) | Afrimine Mararaba'n Jama'a (Younger Granite) |
|---|---|---|
| Mean UCS (MPa) | 142.2 | 190.4 |
| Mean BTS (MPa) | 10.3 | 15.4 |
| Mean Brittleness Index | 0.928 | 0.919 |
| Mean Bulk Density (g/cm³) | 2.62 | 2.68 |
| Mean Specific Gravity | 2.66 | 2.72 |
| Dominant Joint Density | Dense (spacing < 0.3 m) | Sparse (spacing > 1 m) |
| Mean Powder Factor (kg/m³) | 0.573 | 0.495 |
| Mean X50 (mm) | 213 | 460 |
| Mean Uniformity Index n | 1.47 | 1.18 |

**Table 6. Proposed optimised site-specific blast design recommendations.**

| Parameter | JCC Mista Ali (Recommended) | Afrimine Mararaba'n Jama'a (Recommended) |
|---|---|---|
| Burden (m) | 3.0 | 2.8 |
| Spacing (m) | 3.2 | 3.0 |
| Hole Depth (m) | 10.0 | 10.5 |
| Hole Diameter (mm) | 89 | 89 |
| Powder Factor (kg/m³) | 0.55 – 0.58 | 0.60 – 0.65 |
| Target X50 (mm) | 250 – 300 | 350 – 400 |
| Stemming Length (m) | 2.5 | 2.5 |
| Initiation Sequence | Row-by-row, 42 ms inter-row delay | Row-by-row, 42 ms inter-row delay |
| Key Rationale | Moderate PF adequate; dense joints assist fragmentation | Higher PF required to overcome high UCS and sparse jointing |

Note: the Target X50 row defines an acceptable design tolerance band for each site, not a numerical goal to be approached from a coarser starting point. At JCC, the current mean X50 (213 mm) already lies below this band, and the recommendation is to hold current practice within this tolerance for consistency, not to coarsen fragmentation toward it; at Afrimine, by contrast, the current mean X50 (460 mm) lies well above its target band, and the recommended parameter changes are intended to bring fragmentation down into that range.

At JCC Mista Ali, the existing design (mean X50 = 213 mm, n = 1.47) is already adequate because the dense joint network performs much of the fragmentation work; the recommendation is therefore to maintain the powder factor at 0.55 to 0.58 kg/m³ and standardize burden at 3.0 m to reduce inter-blast variability, rather than to increase explosive energy further. At Afrimine Mararaba'n Jama'a, the current powder factor of 0.495 kg/m³ is inadequate for a formation with a mean UCS of 190.4 MPa and sparse jointing; an increase to 0.60 to 0.65 kg/m³ (21 to 31% above current levels), combined with a reduced burden of 2.8 m, is recommended to raise the achievable X50 toward a more crusher-compatible range of 350 to 400 mm. As this study monitored only two blasts per site, these recommended values should be treated as calibration starting points to be validated through trial blasting with continued WipFrag monitoring, rather than as finalised design prescriptions. As the monitoring programme at each site is extended, the larger dataset would also enable the more comprehensive, data-driven empirical and machine-learning-based fragmentation models emerging in recent literature [24,25] to be calibrated and cross-checked against Kuz-Ram for these formations, offering a route to progressively replace the present engineering-judgement adjustments with model-derived optima.

A practical question is how these recommendations can be adopted by quarries such as JCC and Afrimine, which typically operate with limited budgets and technical resources. None of the proposed adjustments requires new capital equipment: they involve reallocating existing explosive within the current charge and adjusting drill pattern geometry within the range already used on site, so implementation costs are expected to be limited primarily to incremental explosive consumption at Afrimine and closer supervision of drilling geometry at both sites.

A phased approach is recommended: first, trial the revised powder factor and burden on a small number of blasts while continuing WipFrag monitoring, using low-cost handheld photography rather than specialised equipment; second, compare fragmentation, secondary breakage, and loading productivity against the pre-trial baseline; and third, adopt the revised parameters as standard practice only once a consistent improvement is confirmed over several blasts. This phased, low-cost validation approach is intended to make the recommendations achievable within the resource constraints typical of these operations, rather than requiring a large upfront investment in blast redesign.

## 4. Conclusions

This comparative case study indicates that intact rock strength and rock mass joint density are associated with, and are the most plausible primary controls on, the contrasting blast fragmentation outcomes observed at two geologically distinct granite formations in Plateau State, Nigeria. The Younger Jurassic granite at Afrimine Mararaba'n Jama'a is significantly stronger and, based on qualitative field assessment, more sparsely jointed than the Precambrian granitic gneiss at JCC Mista Ali ($p < 0.001$ and large effect sizes, $|\text{Cohen's } d| \geq 2.98$, for all measured intact rock parameters), and despite being blasted at a lower powder factor and comparable or smaller burden and spacing, it produced markedly coarser and less uniform fragmentation. The near-perfect correlation between UCS and BTS across the pooled dataset ($r = 0.998$, $p < 0.001$) confirms the internal consistency of the laboratory dataset and indicates that either parameter can serve as a reliable proxy for intact strength in these formations, while also reflecting, in part, the clear separation between the two site populations.

Because only two production blasts were monitored at each site, these fragmentation findings should be read as a site-level association observed in a preliminary comparative case study, rather than as a statistically established causal relationship; they nonetheless indicate that a uniform blast design applied across both formations is unlikely to be either scientifically justified or operationally efficient. On this basis, trialling an increase in powder factor at Afrimine toward 0.60–0.65 kg/m³, while maintaining current practice at JCC with improved geometry consistency, is recommended as a starting point for further monitored trial blasting rather than as a finalised design change. This work provides an ISRM-standardised geomechanical dataset and a preliminary, statistically characterised geomechanical-fragmentation association for these specific Plateau State granite formations, contributing both a practical, low-cost blast-design starting point for the two quarries studied and a quantitative addition to the sparse literature on African granite geomechanics.

Future work should prioritise expanding the monitored-blast dataset at both sites to permit formal inferential testing of the fragmentation comparison, complementing the present qualitative joint-density assessment with a quantitative discontinuity survey, and separating the contributions of blast geometry, powder factor, and rock properties through a more fully factorial monitoring design. Extending the same paired intact-rock/rock-mass/fragmentation framework to other lithologies present in Nigerian and wider West African quarrying, such as basalt and marble, would help to establish the external validity of the relationships identified here and build a broader comparative basis for geomechanically informed blast design across rock types.

## Acknowledgement

The authors gratefully acknowledge the management and staff of Jolex Construction Company, Mista Ali, and Afrimine Construction Company, Mararaba'n Jama'a, for granting access to their quarry sites and production blast data, and the Department of Mining Engineering, University of Jos, for laboratory testing facilities. This research received no specific grant from any funding agency in the public, commercial, or not-for-profit sectors.

## Conflict of Interest

The authors declare that they have no known competing financial interests or personal relationships that could have appeared to influence the work reported in this paper.

## References

[1]. Obaje, N. G. (2009). *Geology and mineral resources of Nigeria* (Lecture Notes in Earth Sciences, Vol. 120). Springer.

[2]. Rahaman, M. A. (1988). Recent advances in the study of the basement complex of Nigeria. In *Precambrian Geology of Nigeria* (pp. 11–43). Geological Survey of Nigeria.

[3]. Turner, D. C. (1976). Structure and petrology of the Younger Granite ring complexes. In C. A. Kogbe (Ed.), *Geology of Nigeria* (pp. 143–158). Elizabethan Press.

[4]. Choudhary, B. S., Sonu, K., Kishore, K., & Anwar, S. (2016). Effect of rock mass properties on blast-induced rock fragmentation. *International Journal of Mining and Mineral Engineering*, *7*(2), 89–101.

[5]. Mehrdanesh, A., Monjezi, M., & Sayadi, A. R. (2018). Evaluation of effect of rock mass properties on fragmentation using robust techniques. *Engineering with Computers*, *34*(2), 253–260.

[6]. Azizi, A., & Moomivand, H. (2021). A new approach to represent impact of discontinuity spacing and rock mass description on the median fragment size of blasted rocks using image analysis of rock mass. *Rock Mechanics and Rock Engineering*, *54*(2), 769–779.

[7]. Hoek, E., & Brown, E. T. (1997). Practical estimates of rock mass strength. *International Journal of Rock Mechanics and Mining Sciences*, *34*(8), 1165–1186.

[8]. Saliu, M. A., & Idowu, K. A. (2014). Investigating the effect of fracture on rock fragmentation efficiency: A case study of Kopec Granite Quarries, South Western Nigeria. *Journal of Earth Sciences and Geotechnical Engineering*, *4*(4), 53–59.

[9]. Idowu, K. A., Olaleye, B. M., & Saliu, M. A. (2021). Application of Split-Desktop image analysis and Kuz-Ram empirical model for evaluation of blast fragmentation efficiency in a typical granite quarry. *Ghana Mining Journal*, *21*(1), 45–52.

[10]. Otokiti, M. O., & Adebayo, B. (2024). Evaluation of rock and explosive properties for fragmentation characterization: An application of WipFrag. *International Journal of Engineering and Advanced Technology Studies*, *12*(1), 13–32.

[11]. Alaba, O. C., Adeniyi, T. O., & Agbalajobi, S. A. (2017). Determination of rock discontinuity for prediction of blasting performances using quantitative and qualitative parameters. *Daffodil International University Journal of Science and Technology*, *12*(1), 85–91.

[12]. Akinola, A. P., Achuenu, I., & Judith, A. A. (2025). Comparative analysis between Afrimine Quarry and Jolex Construction sited in Jos, Plateau State, Nigeria, with respect to unit production cost in order to establish the viability of quarry business. *Frontiers in Economics & Policy Modeling*, *1*(2), 35–51.

[13]. Widzyk-Capehart, E., & Lilly, P. (2002). A review of general considerations for assessing rock mass blastability and fragmentation. *Fragblast*, *6*(2), 151–168.

[14]. Lilly, P. A. (1986). An empirical method of assessing rock mass blastability. In *Proceedings of the Large Open Pit Mining Conference* (pp. 89–92). The Australasian Institute of Mining and Metallurgy.

[15]. Dotto, M. S., & Pourrahimian, Y. (2024). The influence of explosive and rock mass properties on blast damage in a single-hole blasting. *Mining*, (1), 168–188.

[16]. Kuznetsov, V. M. (1973). The mean diameter of the fragments formed by blasting rock. *Soviet Mining Science*, *9*(2), 144–148.

[17]. Cunningham, C. V. B. (2005). The Kuz-Ram fragmentation model – 20 years on. In *Brighton Conference Proceedings 2005* (pp. 201–210). European Federation of Explosives Engineers.

[18]. Ulusay, R., & Hudson, J. A. (Eds.). (2007). *The complete ISRM suggested methods for rock characterization, testing and monitoring: 1974–2006*. ISRM Turkish National Group.

[19]. Shehu, S. A., Yusuf, K. O., & Hashim, M. H. M. (2020). Comparative study of WipFrag image analysis and Kuz-Ram empirical model in granite aggregate quarry and their application for blast fragmentation rating. *Geomechanics and Geoengineering*, *17*(1), 197–205.

[20]. Njock, M. C., Melii, J. L., Poufonne, Y. K., Koffi, Y., Djeuda Tchapnga, H. B., Bilong, P., & Mvondo Ondoa, J. (2021). Influence of natural discontinuities and mechanical properties on the fragmentation of marble by blasting in Central Africa. *Environmental Earth Sciences*, *80*(18), Article 632.

[21]. Sellers, E. J., Fathi Salmi, E., Usami, K., & Walton, G. (2019). Detailed rock mass characterization – a prerequisite for successful differential blast design. In *Proceedings of the 5th ISRM Young Scholars' Symposium on Rock Mechanics and REIF2019 - International Symposium on Rock Engineering for Innovative Future.* ISRM, Okinawa, Japan.

[22]. Erarslan, N., & Ghamgosar, M. (2014). Fracturing and indirect tensile strength of brittle and ductile rocks. In *Rock Engineering and Rock*

*Mechanics: Structures in and on Rock Masses (Proceedings of EUROCK 2014, ISRM European Regional Symposium, Vigo, Spain)* (pp. 812-819). CRC Press.

[23]. Moomivand, H., & Vandyousefi, H. (2020). Development of a new empirical fragmentation model using rock mass properties, blasthole parameters, and powder factor. *Arabian Journal of Geosciences*, *13*(22), Article 1173. https://doi.org/10.1007/s12517-020-06110-2

[24]. Moomivand, H., & Gheybi, M. (2024). Novel empirical models to assess rock fragment size by drilling and blasting. *Measurement*, *238*, Article 115375. https://doi.org/10.1016/j.measurement.2024.115375

[25]. Nourian, A., & Moomivand, H. (2020). Development of a new model to predict uniformity index of fragment size distribution based on the blasthole parameters and blastability index. *Journal of Mining Science*, *56*(1), 47–58. https://doi.org/10.1134/S1062739120016478

[26]. Batouche, T., Tabet, A., Zerzour, O., Hadji, R., Benyoucef, A. A., Moueri, A., & Dinar, H. (2024). Optimizing rock fragmentation in open pit mining: Blasting plan refinement using WipFrag and Kuz-Ram method. *Geomatics, Landmanagement and Landscape*.

[27]. Taiwo, B. O., Gebretsadik, A., Abbas, H. H., Khishe, M., Fissha, Y., Kahraman, E., & Akinlabi, A. A. (2024). Explosive utilization efficiency enhancement: An application of machine learning for powder factor prediction using critical rock characteristics. *Heliyon*, *10*(12).

[28]. Zhang, F., Yang, L., Hu, Y., Ma, J., Liu, N., & Yang, R. (2025). Experimental and numerical study on mechanical response mechanism of granite under coupled confining pressure and blasting load. *Rock Mechanics and Rock Engineering*, *58*(2), 1617–1637.

[29]. Tabet, A., Zezour, O., Dinar, H., Batouche, T., Ben Youcef, A. A., Moussaoui, M., & Lamouri, B. (2026). Optimization of the powder factor during rock masses blasting according to their intrinsic properties. *International Journal of Mining and Geo-Engineering*, *60*(2), 161–170.

[30]. Adesida, P. A., & Salawudeen, W. A. (2026). Assessment of the influence of mechanical properties and mineralogical composition on fragmentation of selected granitic rocks. *FUTA Journal of Engineering and Engineering Technology*, *20*(1), 29–41.

[31]. Saadati, M., Forquin, P., Weddfelt, K., Larsson, P. L., & Hild, F. (2015). A numerical study of the influence from pre-existing cracks on granite rock fragmentation at percussive drilling. *International Journal for Numerical and Analytical Methods in Geomechanics*, *39*(5), 558–570

انجمن مهندسی معدن ایران
نشریه مهندسی معدن و محیط زیست
نشانی نشریه: www.jme.shahroodut.ac.ir
دانشگاه صنعتی شاهرود

# عوامل ژئومکانیکی و تراکم درزه‌ها در خردایش ناشی از انفجار: مطالعه‌ای تطبیقی بر روی معادن سنگ‌شکنِ گنیس گرانیتیِ متعلق به دوران پیش‌کامبرین و گرانیت‌های جوان‌تر در ایالت پلاتو، نیجریه

آیوبامی جاشوا آدگبویه* و کایوده آگوستین ایدووو

گروه مهندسی معدن، دانشکده مهندسی، دانشگاه جاس، شهر جاس، ایالت پلاتو، نیجریه

**اطلاعات مقاله**

**تاریخ ارسال**: ۲۰۲۶/۰۶/۰۱
**تاریخ داوری**: ۲۰۲۶/۰۸/۰۳
**تاریخ پذیرش**: ۲۰۲۶/۰۹/۰۵

DOI: 10.22044/jme.2026.17933.3570

**کلمات کلیدی**

خردایش ناشی از انفجار
ویژگی‌های ژئومکانیکی
گرانیت
WipFrag
مقاومت فشاری تک‌محوره

**چکیده**

انفجار معادن در ایالت پلاتو، نیجریه، معمولاً از طرح‌های کلی و نامشخص در محل معدن پیروی می‌کند که تضاد زمین‌شناسی قابل توجه بین گنیس گرانیتی پرکامبرین میستا علی و گرانیت ژوراسیک جوان‌تر ماراربا جاما را نادیده می‌گیرد. این مطالعه اولین مقایسه کمی و استاندارد شده توسط ISRM از خواص ژئومکانیکی سنگ بکر، چگالی درزه ارزیابی شده میدانی و خردایش پس از انفجار بین این دو سازند را ارائه می‌دهد. مقاومت فشاری تک محوری (UCS)، مقاومت کششی برزیلی (BTS)، چگالی حجمی، وزن مخصوص و شاخص شکنندگی برای ده نمونه در هر محل ($n = 20$) تعیین شد. خردایش پس از انفجار از دو انفجار تولیدی تحت نظارت در هر محل با تجزیه و تحلیل تصویر WipFrag مشخص شد. گرانیت جوان‌تر به طور قابل توجهی میانگین UCS (۱۹۰.۴ در مقابل ۱۴۲.۲ مگاپاسکال) و BTS (۱۵.۴ در مقابل ۱۰.۳ مگاپاسکال؛ $p < 0.001$، Cohen's $d > 4.3$) بالاتری داشت، در حالی که مشاهدات میدانی، درزه‌داری عمدتاً پراکنده را در آن محل در مقابل درزه‌داری متراکم در محل گنیس ثبت کرد. محل گنیس (ضریب پودر ۰.۵۷۳ کیلوگرم بر متر مکعب) تکه‌تکه شدن ریزتر و یکنواخت‌تری ($X50 = 213$ میلی‌متر، $n = 1.47$) نسبت به محل گرانیت (ضریب پودر ۰.۴۹۵ کیلوگرم بر متر مکعب؛ $X50 = 460$ میلی‌متر، $n = 1.18$) ایجاد کرد، ارتباطی که با تأثیر ترکیبی مقاومت دست نخورده و چگالی درزه سازگار است. UCS و BTS تقریباً به طور کامل در مجموعه داده‌های جمع‌آوری شده همبستگی داشتند ($r = 0.998$). از آنجا که تنها دو انفجار در هر سایت مورد بررسی قرار گرفت، این مطالعه به عنوان یک مطالعه موردی مقایسه‌ای اولیه ارائه شده است، نه یک رابطه علی و معلولی آماری. یافته‌ها از آزمایش افزایش ضریب پودر (۰.۶۰–۰.۶۵ کیلوگرم بر متر مکعب) در سایت گرانیتی پشتیبانی می‌کنند و یک مجموعه داده ژئومکانیکی مبتنی بر مکانیک را ارائه می‌دهند که در حال حاضر برای سازندهای گرانیتی آفریقا کمیاب است.

نویسنده مسئول مکاتبات: adegboyea@unijos.edu.ng (الف. ج. آدگبویه)